

# BASIC–LIVER, PANCREAS, AND BILIARY TRACT

## Glibenclamide Stimulates Fluid Secretion in Rodent Cholangiocytes Through a Cystic Fibrosis Transmembrane Conductance Regulator–Independent Mechanism

CARLO SPIRÌ,<sup>\*,†,§</sup> ROMINA FIOROTTO,<sup>\*,†</sup> LEI SONG,<sup>¶</sup> JOSEPH SANTOS–SACCHI,<sup>¶</sup> LAJOS OKOLICSANYI,<sup>||</sup> SARA MASIER,<sup>\*</sup> LORETTA ROCCHI,<sup>#</sup> MARIA PIA VAIRETTI,<sup>\*\*,†</sup> MARINA DE BERNARD,<sup>†,††</sup> SAIDA MELERO,<sup>||</sup> TULLIO POZZAN,<sup>†</sup> and MARIO STRAZZABOSCO<sup>\*,†,§</sup>

<sup>\*</sup>Department of Medical and Surgical Sciences, University of Padova, Padova, Italy; <sup>†</sup>Venetian Institute of Molecular Medicine, Padova, Italy; <sup>§</sup>Division of Gastroenterology and Center for Liver Research, Ospedali Riuniti di Bergamo, Bergamo, Italy; <sup>¶</sup>Departments of Surgery and Neurobiology, Yale University School of Medicine, New Haven, Connecticut; <sup>||</sup>Department of Surgical and Gastroenterological Sciences, University of Padova, Padova, Italy; <sup>#</sup>Department of Forensic Medicine, University of Pavia, Pavia, Italy; <sup>\*\*</sup>Department of Internal Medicine and Medical Therapy, University of Pavia, Pavia, Italy; and <sup>††</sup>Department of Biology, University of Padova, Padova, Italy

**Background & Aims:** Progressive liver disease is a severe complication of cystic fibrosis, a genetic disease characterized by impaired epithelial adenosine 3',5'-cyclic monophosphate–dependent secretion caused by mutations in the cystic fibrosis transmembrane conductance regulator (CFTR). In the liver, CFTR is expressed in cholangiocytes and regulates the fluid and electrolyte content of the bile. Glibenclamide, a sulfonylurea and a known CFTR inhibitor, paradoxically stimulates cholangiocyte secretion. We studied the molecular mechanisms underlying this effect and whether glibenclamide could restore cholangiocyte secretion in cystic fibrosis. **Methods:** NRC-1 cells, freshly isolated rat cholangiocytes, isolated rat biliary ducts, and isolated biliary ducts from CFTR-defective mice (Cftr<sup>tm1Unc</sup>) were used to study fluid secretion (by video-optical planimetry), glibenclamide-induced secretion (by high-performance liquid chromatography in cell culture medium), intracellular pH and intracellular Ca<sup>2+</sup> concentration transients [2'7'-bis(2-carboxyethyl)-5,6-carboxyfluorescein-acetoxymethylester and Fura-2 f-AM (5-Oxazolecarboxylic acid, 2-(6-(bis(2-((acetyloxy)methoxy)-2-oxoethyl)amino)-5-(2-(2-(bis(2-((acetyloxy)methoxy)-2-oxoethyl)amino)-5-methylphenoxy)ethoxy)-2-benzofuranyl)-, (acetyloxy)methyl ester) microfluorometry], gene expression (by reverse-transcription polymerase chain reaction), and changes in membrane capacitance (by patch-clamp experiments). **Results:** Stimulation of cholangiocyte secretion by glibenclamide and tolbutamide required Cl<sup>–</sup> and was mediated by the sulfonylurea receptor 2B. Glibenclamide-induced secretion was blocked by inhibitors of exocytosis (colchicine, wortmannin, LY294002, and N-ethylmaleimide) and by inhibitors of secretory granule acidification (vanadate, bafilomycin A1, and niflumic acid) but was Ca<sup>2+</sup> and depolarization independent; membrane capacitance measurements were consistent with stimulation of vesicular transport and fusion. Glibenclamide, unlike secretin and

forskolin, was able to stimulate secretion in Cftr<sup>tm1Unc</sup> mice, thus indicating that this secretory mechanism was preserved. **Conclusions:** The ability of glibenclamide to stimulate secretion in CFTR-defective mice makes sulfonylureas a model class of compounds to design drugs useful in the treatment of cystic fibrosis with liver impairment and possibly of other cholestatic diseases.

The intrahepatic biliary epithelium extensively modifies hepatocellular bile by increasing its water content and HCO<sub>3</sub><sup>–</sup> concentration. Fluidification of bile and its alkalization are required to meet digestive needs and to facilitate the flux of bile. This function of the biliary epithelium is regulated by gastrointestinal hormones and by paracrine signals that act either through the adenosine 3',5'-cyclic monophosphate (cAMP)/protein kinase A pathway (secretin) or via Ca<sup>2+</sup> signaling (purinergic receptors).<sup>1</sup>

Ductal cholestasis, ie, reduced fluid and electrolyte transport by cholangiocytes, is a central step in the pathogenetic sequence of biliary tree diseases, as exemplified by the progressive liver disease associated with cystic fibrosis (CF), a common genetic defect in which a

*Abbreviations used in this paper:* BCECF, 2'7'-bis(2-carboxyethyl)-5,6-carboxyfluorescein-acetoxymethylester; bp, base pair; CF, cystic fibrosis; CFTR, cystic fibrosis transmembrane conductance regulator; C<sub>m</sub>, membrane capacitance; DIDS, 4,4'-diisothiocyanato-stilbene-2,2'-disulfonic acid; DMSO, dimethyl sulfoxide; IBDU, isolated bile duct unit; Kir, inward rectifier K<sup>+</sup> channel; MEM, minimal essential medium; NEM, N-ethylmaleimide; NKCC1, Na-K-2Cl cotransporter isoform 1; NRC-1, normal rat cholangiocyte cell line; pH<sub>i</sub>, intracellular pH; RT-PCR, reverse-transcription polymerase chain reaction; SUR, sulfonylurea receptor; TEA, tetraethylammonium.

© 2005 by the American Gastroenterological Association  
0016-5085/05/\$30.00

doi:10.1053/j.gastro.2005.03.048

failure of cAMP-regulated  $\text{Cl}^-$  transport (CF transmembrane conductance regulator; CFTR) causes a secretory failure in a number of epithelia, including the biliary tree.<sup>2,3</sup> Recently, it was shown that glibenclamide stimulates bile flow at the level of the bile duct epithelium,<sup>4</sup> a result in apparent contradiction to the known inhibitory effects of glibenclamide on CFTR. Progressive pulmonary disease is the leading cause of death in CF, but as the life expectancy for these patients is extended through improved pulmonary, nutritional, and general medical care, hepatobiliary complications become more frequent and have a negative effect on survival. As a consequence of the ductal cholestasis that results from defective biliary  $\text{Cl}^-$  and fluid transport, liver inflammation, cholangiocyte damage, and portal fibrosis progressively occur.<sup>2</sup> Pharmacological improvement of ductal secretion may help to reverse this series of events.

Sulfonylureas are widely used in the treatment of non-insulin-dependent diabetes mellitus (type 2 diabetes) because of their ability to stimulate insulin secretion from pancreatic  $\beta$ -cells.<sup>5</sup> In this study, we investigated the molecular mechanisms that underlie the recently reported choleric effects of glibenclamide on the bile duct epithelium and its possible exploitation in CF. Our results indicate that in isolated bile duct units (IBDUs), sulfonylureas stimulate fluid secretion by a mechanism that is independent of  $\text{Ca}^{2+}$  and cAMP signaling but involves vesicle transport and fusion. The glibenclamide effect is maintained in cholangiocytes isolated from CFTR knockout mice. The stimulatory effect of glibenclamide on cholangiocyte secretion in cells lacking CFTR makes this class of compounds an attractive tool to stimulate fluid secretion in CF liver disease, a prototypic cholangiopathy present in up to 30% of CF patients that seriously affects morbidity and mortality.

## Materials and Methods

### Chemicals and Solutions

Epidermal growth factor, dexamethasone, triiodothyronine, ethylenediaminetetraacetic acid, collagenase IV, collagenase XI, pronase, hyaluronidase, deoxyribonuclease, forskolin, insulin, diethylpicrocarbonate, glibenclamide, 4,4'-diisothiocyanato-stilbene-2,2'-disulfonic acid (DIDS), diazoxide, tolbutamide, tetraethylammonium (TEA), niflumic acid, vanadium oxide, wortmannin, LY294002, colchicine,  $\gamma$ -lumilcolchicine, TRI Reagent (Sigma Chemical Company, Milan, Italy), barium- $\text{Cl}^-$ , adenosine triphosphate (ATP), diButyryl (dB)-cAMP, bafilomycin A1, and nocodazole were purchased from Sigma. Culture media,  $\alpha$ -minimal essential medium (MEM), Dulbecco's MEM, Ham's F12, fetal bovine serum, MEM nonessential amino acid solution, MEM vitamin solutions, glyceryl monostearate, chemically defined lipid concentrate, soybean trypsin inhibitor, penicillin/streptomycin,

gentamicin, trypsin/ethylenediaminetetraacetic acid, and glutamine were purchased from Gibco (Life Technology, Milano, Italy). NuSerum and bovine pituitary extract were obtained from Becton Dickinson (Milan, Italy). Membrane inserts were purchased from Nunc (Mascia Brunelli, Milan, Italy), and Dynabeads M-450 rat anti-mouse immunoglobulin M was purchased from Deutsche Dynal GmbH (Hamburg, Germany). 2'7'-Bis(2-carboxyethyl)-5,6-carboxyfluorescein-acetoxymethylester (BCECF) and Fura-2 were purchased from Molecular Probes (Eugene, OR). Moloney murine leukemia virus reverse transcriptase was obtained from Perkin Elmer (Milan, Italy), whereas a Qiagen QIAquick PCR Purification Kit and Qiagen QIAquick Gel Extraction Kit were purchased from Qiagen GMBM (Ilden, Germany). Anti-*Taq* DNA polymerase antibody was obtained from Clontech (Milano, Italy). The composition of perfusion buffers used was essentially as described previously.<sup>3,6</sup> In HEPES used to acid load cells, 20 mmol/L  $\text{NH}_4\text{Cl}$  was substituted for equal amounts of NaCl. BCECF, Fura-2-AM, glibenclamide, diazoxide, bafilomycin A1, wortmannin, and LY294002 were prepared as a 1 mmol/L stock solution dissolved in dimethyl sulfoxide (DMSO), whereas nigericin was solubilized in ethanol.

### Glibenclamide Secretion in NRC-1 Cell Culture and in Isolated and Perfused Rat Liver

NRC-1 is a well-differentiated normal rat cholangiocyte cell line that maintains a polarized distribution of membrane markers and ion transporters and has been extensively characterized and used.<sup>7-9</sup> Cells were grown as previously described<sup>7-9</sup> over collagen-coated semipermeable membrane inserts (Nunc, Mascia-Brunelli, Milano, Italy). Experiments were performed in cells cultured for 1 week after they reached confluence and had a transepithelial resistance  $>1000 \Omega/\text{cm}^2$  (Millicell-ERS System; Millipore Co, Bedford, MA).<sup>7</sup> NRC-1 monolayers were exposed to glibenclamide from basolateral side, and at different times, apical supernatant was collected.

Animals received care according to the principles outlined in the *Guide for the Care and Use of Laboratory Animals* (National Academy Press, 1996, 7th edition), and the following protocols were approved by the University of Padua Institutional Veterinary Medicine Service. Sprague-Dawley rats were anesthetized with pentobarbital (50 mg/kg body weight); procedures for isolated and perfused rat liver and setup were performed as previously described.<sup>10</sup> Bile flow was measured gravimetrically in preweighted tubes, and perfusion pressure was monitored continuously. Liver viability was ascertained by monitoring perfusion pressure and oxygen consumption during the course of the experiment and by determining trypan blue distribution on completion.

Glibenclamide and its 2 major metabolites (4-*trans*- and 3-*cis*-hydroxyglibenclamide) were measured by high-performance liquid chromatography in the bile collected from isolated and perfused rat liver or in the supernatant of NRC-1 cell line. Gliclazide (0.1–10  $\mu\text{g}$ ) was used as an internal standard. Sulfuric acid 1N was added to bile or to cell supernatant, and, after the addition of *N*-hexane/ethyl acetate (3:1, vol/vol), the

organic phase was dried, dissolved in mobile phase, and injected into a liquid chromatographic system (Agilent Series 1100; Hewlett-Packard, Palo Alto, CA). The analytical column was a reversed-phase LiChrospher RP-Select B obtained from Merck (Darmstadt, Germany). Calibration standard samples were prepared by adding glibenclamide or metabolites to "blank" bile or, in the case of cell overnatants, to a buffer solution. Calibration lines of all analytes were linear in the range investigated: correlation coefficient values ( $r^2$ ) were consistently  $>0.9834$ . The mobile phase (flow at 1 mL/min) consisted of a mixture of acetonitrile and water (50:50, vol/vol) containing sodium dodecylsulfate (0.01 mol/L) and glacial acetic acid (0.5% vol/vol). The UV detection wavelength was 230 nm.

### Intrahepatic Rat Bile Duct Units and Immunopurified Bile Duct Cells

Rats and mice were anesthetized as described previously. IBDUs (ie, sealed fragments of isolated bile ductules in short-term culture that have retained polarity and secrete into a closed lumen) were prepared and purified as previously described<sup>6,11,12</sup>; they were plated for 24 hours over a thin layer of Matrigel (Collaborative Research Products, Bedford, MA) as previously described.<sup>6,11,12</sup> Immunomagnetic isolation of cholangiocytes was performed as previously described<sup>13</sup> by using the OC-2 primary antibody (1:1000; a kind gift of Dr D. Hixson, Brown University, Providence, RI). Histochemical assays for  $\gamma$ -glutamyltranspeptidase indicated purity values of  $>95\%$  in all cholangiocyte preparations used. Viability was evaluated by trypan blue exclusion.

### Assessment of Ductular Secretion in Intrahepatic Rat Bile Duct Units by Video-optical Planimetry

Expansion of the IBDU lumen over time was quantified by video-optical planimetry as a measure of the ductular secretion rate, as previously described.<sup>6,11,12</sup> After a 5-minute baseline period, IBDUs were exposed to glibenclamide (100  $\mu$ mol/L), to tolbutamide (100  $\mu$ mol/L), or to glibenclamide and different inhibitors; the luminal area was then measured every 5 minutes for up to 30 minutes. Serial images of the IBDU were acquired by a JVC TKC 1380 video camera (Galileo Siscam, Firenze, Italy); luminal areas were determined from the recorded images by using an image processor (Arkon; Nikon; Firenze, Italy).

### Measurement of Na-K-2Cl Cotransporter Isoform 1 Activity

The effects of glibenclamide on the activity of the  $\text{Na}^+/\text{K}^+/\text{2Cl}^-$  cotransporter was assessed by measuring the recovery of intracellular pH (pHi) from  $\text{NH}_4\text{Cl}^-$ -induced alkalization by using the cell-permeant fluorescent pHi indicator BCECF/AM (12  $\mu$ mol/L). BCECF loading procedures of IBDU, the microscopic setup, and the measurement and calibration procedures have already been described.<sup>14</sup> Acid and

base fluxes were calculated by using cellular intrinsic and total buffering powers ( $\beta_i$  and  $\beta_{\text{tot}}$ , respectively), values previously measured.<sup>6,11</sup> The rates of pHi changes ( $\delta\text{pHi}/\delta t$ ) were calculated as previously described.<sup>6,11</sup> The effects of glibenclamide on  $\text{Na}^+/\text{K}^+/\text{2Cl}^-$  activity were assessed by measuring the rate of pHi recovery from an alkaline load induced by 20 mmol/L  $\text{NH}_4^+\text{Cl}^-$ .<sup>6,15</sup> The  $\text{Na}^+/\text{K}^+/\text{2Cl}^-$  cotransporter can transport  $\text{NH}_4^+$  in stoichiometrical substitution of  $\text{K}^+$ . When cells are exposed to  $\text{NH}_4\text{Cl}$ ,  $\text{NH}_3$  enters the cells by nonionic diffusion and leads to cytoplasmatic alkalization. The subsequent cellular uptake of  $\text{NH}_4^+$  by Na-K-2Cl cotransporter isoform 1 (NKCC1) causes pHi acidification, and NKCC1 activity can be measured from the initial phase of the acidification slope.<sup>6,15</sup>

### Measurement of Intracellular $\text{Ca}^{2+}$

Intracellular  $\text{Ca}^{2+}$  transients were measured by using Fura-2-AM. IBDUs were loaded in tissue culture medium for 20–30 minutes at room temperature with Fura-2-AM (5  $\mu$ mol/L). Coverslips with dye-loaded cells were mounted into a heated metal flow-through perfusion chamber, placed on the stage of an inverted Olympus IX 70 microscope (Milano, Italy), and perfused by gravity feed at 1.5–2 mL/min. After a 3-minute baseline period, cells were exposed to glibenclamide (100  $\mu$ mol/L) for 10 minutes, and at the end of the experiment, ATP (10  $\mu$ mol/L) was used as an internal control. Emitted fluorescence was measured in response to alternate pulses of excitation light (10 milliseconds long) at 340 and 380 nm. The emitted fluorescence (510 nm) was focused on a photomultiplier tube, amplified, digitally converted, and analyzed with Till Vision software (Till Photonics, Martinsried, Germany). Images of the IBDU were acquired by a charge-coupled device camera. The ratio of emitted light from the 2 excitation wavelengths (340 and 380 nm) of Fura-2 provides a measure of ionized cytoplasmic  $[\text{Ca}^{2+}]$ .<sup>16</sup>

### Sulfonylurea Receptor, Inward Rectifier $\text{K}^+$ Channel 6.x, and chloride channels (CLC)-3 Gene Expression

Sulfonylurea receptor (SUR) and inward rectifier  $\text{K}^+$  channel (Kir) 6.x isoforms and chloride channels (CLC)-3 gene expression were assessed by reverse-transcription polymerase chain reaction (RT-PCR). SUR1 messenger RNA (mRNA) was detected by using the primers 5'-GCAGCCGAGAGCGAGGAA-GATGA-3' and 5'-ACAGCCAGGGCGGAGACACAGAGT-3', which amplified a 539-base pair (bp) fragment. SUR2 mRNA was amplified by using the primers 5'-CGCGGCGGT-CATCGTGCTC-3' and 5'-CGCCGCGCCTGCTCGTAGTT-3', which amplified a 603-bp fragment. SUR2AB mRNA was detected by using the primers 5'-GACAGCCTTTGCG-GATCG-3' and 5'-GCATCGAGACACAGGTGCTG-3', which amplified a 387-bp fragment for SUR2A and a 211-bp fragment for SUR2B. CLC-3 mRNA was detected by using the primers 5'-GCGAGAAAAGTGTAAGGAC-3' and 5'-TCAAAGC-CCAAAAGATGTA-3', which amplified a 377-bp fragment; Kir 6.1 mRNA was detected by using the primers 5'-TTCTGCG-TTCTCTTCTCCATCG-3' and 5'-GGGGCTACGCTTAT-

CAATCACAT-3', which amplified a 445-bp fragment. Kir 6.2 mRNA was detected by using the primers 5'-GGAGAG-GAGGGCCCGCTTCGTGTC-3' and 5'-GGCGTAATGAT-CATGCTTTTCGGAGGTC-3', which amplified a 553-bp fragment; 28S mRNA was detected by using the primers 5'-AGAAGGGCAAAGCTCGCTT-3' and 5'-AGCAGGAT-TACCATGGCAAC-3', which amplified a 288-bp fragment. Total RNA was isolated from OC-2 using the TRI Reagent solution (Sigma), according to the manufacturer's instructions. One microgram of total RNA was reverse-transcribed with Moloney murine leukemia virus reverse transcriptase (2.5 U/ $\mu$ L). PCR was performed in a thermocycler M. J. Research (M-Medical, Firenze, Italy) with AmpliTaq Gold polymerase and 1 $\times$  GeneAmp buffer (Applied Biosystems Inc, Foster City, CA). PCR was initiated by hot start, followed by 40 cycles of 94°C for 1 minute, 50°C–74°C for 1 minute, and 72°C for 1 minute and by a final extension at 72°C for 10 minutes. Contamination by genomic DNA was ruled out by running samples without a previous RT-PCR phase. Preliminary kinetic analysis was performed to position amplification cycles on the exponential phase of the reaction. Amplification products were electrophoresed on 7% acrylamide gel, visualized by ethidium bromide, and then silver-stained. Purified PCR products were sequenced on an ABI 373A Stretch automated sequencer (Perkin-Elmer, Milan, Italy) to verify the identity.

### Patch-Clamp Experiments

Immunopurified cholangiocytes were identified with a Nikon Eclipse E600FN microscope by visualizing antibody-coated magnetic beads (4.5  $\mu$ m) bound to the cell-surface antigens. The cells were whole-cell voltage-clamped with an Axopatch 200B amplifier and Digidata 1320A board (Axon Instruments, Union City, CA) by using solutions modified from Barg et al.<sup>17</sup> Extracellular medium contained (mmol/L) NaCl 138, KCl 5, MgCl<sub>2</sub> 1.2, CaCl<sub>2</sub> 2.6, and HEPES 5. The pH was adjusted to 7.4 with NaOH, and osmolarity was adjusted to 310 mOsm with D-glucose. Pipette solution contained (mmol/L) K<sup>+</sup>-gluconate 125, KCl 10, NaCl 10, MgCl<sub>2</sub> 1, HEPES 5, ethylene glycol-bis( $\beta$ -aminoethyl ether)-N,N,N',N'-tetraacetic acid 10, CaCl<sub>2</sub> 5 (170 nmol/L free Ca<sup>2+</sup>), and Mg-ATP 3; pH was adjusted to 7.15 with KOH. The solution had an osmolarity of approximately 310 mOsm. DMSO was used to dissolve tolbutamide and nocodazole before their addition into the pipette solution.  $\gamma$ -Lumicolchicine was prepared in chloroform. The final concentration of DMSO and chloroform in pipette solutions was 0.1%. Some cells were pretreated with colchicine (50  $\mu$ mol/L),  $\gamma$ -lumicolchicine (50  $\mu$ mol/L), and nocodazole (10  $\mu$ mol/L) in extracellular medium for 30, 30, and 60 minutes, respectively.

Membrane capacitance ( $C_m$ ) measurements were begun immediately after the establishment of a whole-cell recording condition. Holding potentials of -40 and -80 mV did not provide stable recordings, and it proved difficult to hold the cells for the required prolonged recording periods. Consequently, cells were typically held at 0 mV during  $C_m$  measurements. The initial pipette resistance was 4–7 M $\Omega$ . Gigohm seals were obtained (1.5–3.5 G $\Omega$ ), and stray capaci-

tance was compensated before the rupture of the cell membrane. Uncompensated series resistances ranged from 10 to 30 M $\Omega$  and remained uncompensated, because the capacitance measurement algorithm is sensitive to introduced system lag. Corrections for series resistance were subsequently made off-line. Capacitance was tracked (every 150 milliseconds) with a high-resolution dual sinusoidal (10-mV peak at both 390.6 and 781.2 Hz) stimulus paradigm.<sup>18,19</sup> Simultaneously, membrane resistance, series resistance, and holding current were recorded. Transient analysis measurements with 10-mV steps were confirmatory. During our measurements, we were careful to record from isolated single cells because cell groups could have been coupled by gap junctions. It is well known that recordings from single cells in a group of coupled cells present an inflated syncytial capacitance, which could be voltage dependent.<sup>20</sup> Another reason for avoiding coupled cell groups is that the use of standard single- and dual-sine measurement approaches is invalidated by a model other than a single resistance-capacitance compartment.<sup>19</sup>

For a subset of cells, current voltage relations were investigated with a voltage step series (-100 to +40 or 50 mV; 200-millisecond step duration; holding potential of -60 mV) that was delivered to cells near the beginning and several times during the continuous monitoring of  $C_m$ . Current voltage (I-V) plots were derived from the last 50 milliseconds of current response.  $C_m$  recordings were made until  $C_m$  stabilized; typical durations ranged from 10 to 20 minutes. Statistical comparisons were made at steady state. A 4-pole Bessel filter at 10 kHz was used. All data acquisition and analyses were performed with the Windows-based voltage clamp software jClamp (SciSoft, New Haven, CT). Digital photos were captured with jClamp.

### Cystic Fibrosis Transmembrane Conductance Regulator Knockout Mice

Congenic B6.129P2-Cftr<sup>tm1Unc</sup> mice, which possess the S489X mutation that blocks transcription of CFTR,<sup>21</sup> were used. Heterozygous breeding pairs were obtained from Jackson Laboratories (Bar Harbor, ME) and then bred in our animal facility. Genotypes for each mouse were determined by PCR with DNA isolated from tail clips by following Jackson Laboratories' instructions. Mice were maintained on a liquid elemental diet (Peptamen; Nestle, Milan, Italy) to prevent the intestinal obstruction associated with the CFTR mutation. Wild-type mice received regular solid mouse chow.<sup>21</sup> Autoclaved tap water in bottles with sipper tubes was provided ad libitum. Mice selected for the experiments reported here were 7 to 8 weeks old without obvious signs of disease or discomfort (average weight, 18  $\pm$  2.3 g for CFTR<sup>-/-</sup> and 22  $\pm$  1.7 g for their normal (CFTR<sup>+/+</sup> and CFTR<sup>+/-</sup>) littermates. For experiments with isolated perfused mouse liver, animals were anesthetized with pentobarbital sodium (50 mg/kg body weight). The abdomen was opened, and the gallbladder was cannulated after distal ligation of the common bile duct.<sup>22</sup> The liver was perfused in situ at 5 mL/min with oxygenated HCO<sub>3</sub><sup>-</sup>-containing Ringer buffer and maintained at 37°C. Bile sampling

was started after a stabilizing period of 10 minutes after cannulation. Bile flow was determined gravimetrically, assuming a density of 1 g/mL for bile.

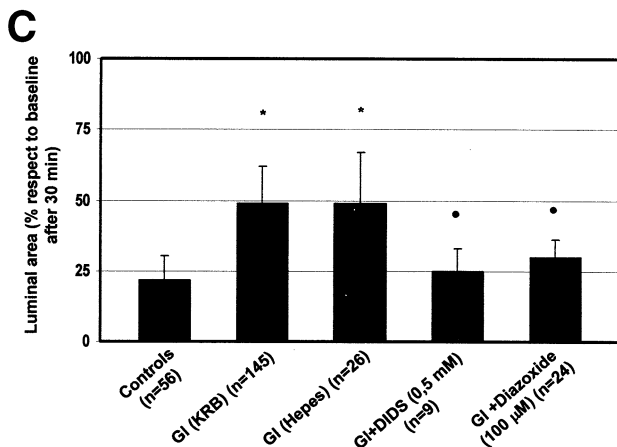
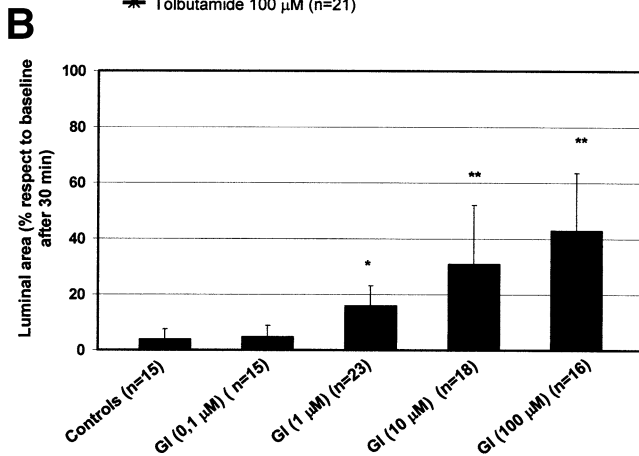
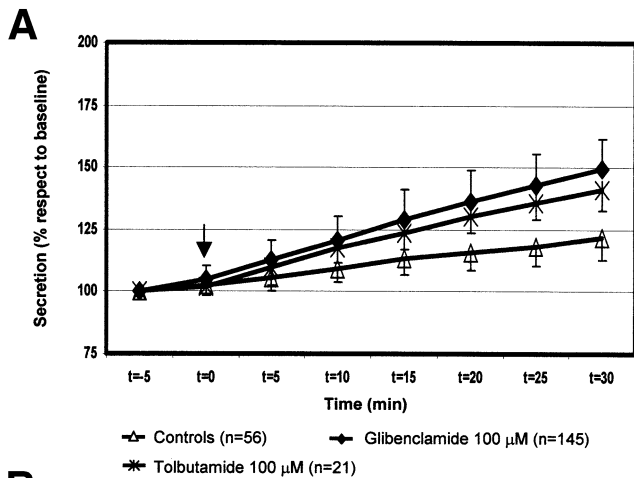
**Statistical Analysis**

Results are shown as mean ± SD. Statistical comparisons were made with Student *t* tests or analysis of variance, with Tukey post hoc tests where appropriate. GraphPad software (Biosoft, Cambridge, UK) was used; *P* values <.05 were considered significant.

**Table 1.** Luminal Area Expansion (Percentage With Respect to Baseline) in IBDUs

Variable	Changes (30 min)	n	<i>P</i>
Controls (KRB)	21 ± 9	56	
Controls (HEPES)	21 ± 11	30	
Glib (KRB)	49 ± 13	145	<.001 vs control
DIDS + glib	24 ± 8	9	<.005 vs glib
Glibenclamide (HEPES)	49 ± 18	26	<.001 vs control
Tolbutamide	41 ± 9	20	<.001 vs control
Diazoxide + glib	30 ± 6	24	<.005 vs glib
Colchicine + glib	24 ± 5	24	<.001 vs glib
γ-Lumilcolchicine + glib	47 ± 7	31	NS vs glib
Wortmannin + glib	21 ± 9	22	<.001 vs glib
LY294002 + glib	19 ± 7	13	<.001 vs glib
NEM + glib	17 ± 7	11	<.01 vs glib
Barium	19 ± 13	12	NS vs control
Tea	22 ± 9	32	NS vs control
Bafilomycin + glib	17 ± 6	8	<.01 vs glib
Vanadate + glib	29 ± 6	20	<.01 vs glib
Niflumic acid	16 ± 5	13	<.001 vs glib

KRB; HCO<sub>3</sub><sup>-</sup> containing Ringer buffer; NS; not significant; glib, glibenclamide.



**Results**

**Glibenclamide-Induced Fluid Secretion in Isolated Bile Duct Units**

Cholangiocyte secretion was measured, as previously described,<sup>4</sup> from the change in luminal area induced by exposure of rat intrahepatic bile duct units to glibenclamide (Figure 1A and Table 1). Administration of glibenclamide induced a dose-dependent (0.1–100 μmol/L) increase in luminal area with respect to controls. The increase in luminal area was 16% ± 7% (*P* < .05) at 1 μmol/L and reached the maximal effect at 100 μmol/L: 45% ± 20% (expressed as percentage increase with respect to baseline after 30 minutes; *P* < .01;

**Figure 1.** Sulfonylureas-stimulated secretion in IBDUs is dose dependent, HCO<sub>3</sub><sup>-</sup> independent, and Cl<sup>-</sup> dependent. (A) IBDUs were examined under control conditions for 10 minutes and then for an additional 30 minutes after the administration of glibenclamide or tolbutamide (arrow). Both sulfonylureas induced a significant (*P* < .001) increase in the luminal area. (B) Glibenclamide stimulates secretion in IBDUs in a dose-dependent manner. Columns represent the percentage of luminal area expansion with respect to baseline after 30 minutes of glibenclamide administration (mean ± SD). \**P* < .05 and \*\**P* < .01 vs controls. (C) Perfusion with HCO<sub>3</sub><sup>-</sup>-free buffer (HEPES) did not affect the increase in luminal area induced by glibenclamide, which is inhibited by the Cl<sup>-</sup> transporter inhibitor DIDS. Diazoxide inhibits the choleric effect of glibenclamide. Columns represent the percentage of luminal area expansion with respect to baseline after 30 minutes of glibenclamide administration (mean ± SD). \**P* < .001 vs controls; •*P* < .05 vs glibenclamide. KRB, HCO<sub>3</sub><sup>-</sup>-containing Ringer buffer; GI, glibenclamide.

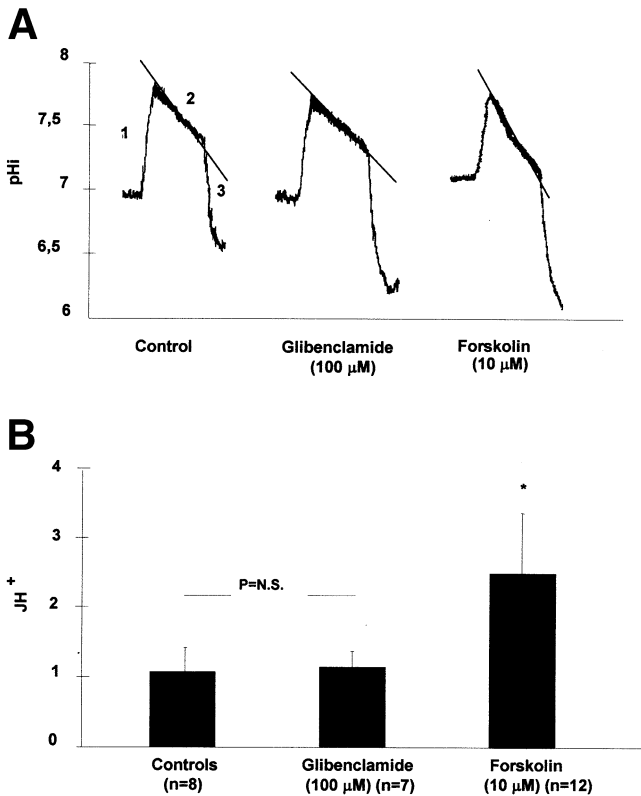


**Figure 2.** Glibenclamide-stimulated secretion in IBDUs does not involve stimulation of the  $\text{Na}^+\text{-K}^+\text{-2Cl}^-$  cotransporter. (A)  $\text{Na}^+\text{/K}^+\text{/2Cl}^-$  activity was measured by using the  $\text{NH}_4\text{Cl}^-$  (20 mmol/L) pulse technique<sup>15</sup> (which exploits the ability of NKCC1 to transport  $\text{NH}_4^+$  in stoichiometrical substitution of  $\text{K}^+$ ) from the initial rate of acidification (120 seconds) (2) after the  $\text{NH}_3$ -induced alkalinization (1); rapid acidification occurred after  $\text{NH}_4\text{Cl}$  withdrawal (3). (B) The graph bars show the transmembrane  $\text{H}^+$  fluxes ( $\text{J}_{\text{H}^+}$ ) calculated as  $\delta\text{pHi}/\delta t \times \beta_i$  (intrinsic buffering power) at pH 7.5. Columns represent the mean  $\pm$  SD. \* $P < .01$  vs controls. N.S., not significant.

Figure 1B). Glibenclamide-induced choleresis was  $\text{Cl}^-$  dependent: it was blocked by bumetanide,<sup>4</sup> an NKCC1 inhibitor, and by DIDS (0.5 mmol/L), a general inhibitor of  $\text{Cl}^-$ -dependent transport (Table 1). Omission of  $\text{HCO}_3^-$  from the perfusate (HEPES buffer), conversely, did not inhibit glibenclamide choleresis (Figure 1C and Table 1), thus indicating that, in contrast to secretory events that depend on cAMP or  $\text{Ca}^{2+}$  signaling,<sup>3,23</sup>  $\text{HCO}_3^-$  transport is likely not involved in glibenclamide choleresis. Contrary to a previous hypothesis based on bumetanide inhibition,<sup>4</sup> direct measurement of NKCC1 activity (Figure 2) showed that glibenclamide did not stimulate NKCC1; on the other hand, forskolin (10  $\mu\text{mol/L}$ ) administration induced the expected stimulatory effect. NKCC1 activity was as follows: transmembrane  $\text{H}^+$  fluxes ( $\text{J}_{\text{H}^+}$ ) =  $1.08 \pm 0.26$   $\text{mmol} \cdot \text{L}^{-1} \cdot \text{min}^{-1}$ ,  $\delta\text{pH}/\delta t = 0.08 \pm 0.01/\text{min}$  (pH 7.5;  $n = 7$ ) in controls;  $\text{J}_{\text{H}^+} = 2.5 \pm 0.88$   $\text{mmol} \cdot \text{L}^{-1} \cdot \text{min}^{-1}$ ,  $\delta\text{pH}/\delta t = 0.171 \pm 0.06/\text{min}$  (pH

7.5;  $n = 12$ ) in IBDU treated with forskolin (10  $\mu\text{mol/L}$ ); and  $\text{J}_{\text{H}^+} = 1.15 \pm 0.23$   $\text{mmol} \cdot \text{L}^{-1} \cdot \text{min}^{-1}$ ,  $\delta\text{pH}/\delta t = 0.074 \pm 0.01/\text{min}$  (pH 7.5;  $n = 8$ ; not significant vs controls) in IBDU treated with glibenclamide.

### Glibenclamide Is Not Secreted by Cholangiocytes

Many drugs induce osmotic bile secretion after their active transport and concentration into the bile. Therefore, we measured the concentration of glibenclamide and of its metabolites 3-*cis*-hydroxyglibenclamide and 4-*trans*-hydroxygliburide in the bile collected from isolated rat livers perfused with 100  $\mu\text{mol/L}$  glibenclamide for 30 minutes and compared it with the concentrations found in the apical overnatant of rat cholangiocyte monolayers after the administration of 100  $\mu\text{mol/L}$  glibenclamide from the basolateral side. The glibenclamide concentration in bile collected from isolated rat livers was  $127 \pm 21$   $\mu\text{mol/L}$  ( $n = 4$ ), whereas that of its metabolites 3-*cis*-hydroxygliburide and 4-*trans*-hydroxygliburide was  $490 \pm 113$   $\mu\text{mol/L}$  and  $311 \pm 86$   $\mu\text{mol/L}$ , respectively. Conversely, after basolateral administration of glibenclamide (100  $\mu\text{mol/L}$ ) to polarized NRC-1 cholangiocyte monolayers, no metabolites were detected in the apical medium, and the glibenclamide concentration linearly increased, reaching only 32.5  $\mu\text{mol/L}$  after a 2-hour incubation (data not shown). This is consistent with diffusion rather than active transport by cholangiocytes. Thus, an osmotic effect by glibenclamide and its metabolites may only partially account for stimulation of hepatocellular bile flow in the isolated perfused rat liver, but not for the secretory effects induced by glibenclamide in isolated cholangiocyte units that are not capable of secreting glibenclamide or its metabolites into the lumen.

### Stimulation of Ductal Choleresis Is a Property of Sulfonylurea Compounds and Is Mediated by Interaction With Cholangiocyte Sulfonylurea Receptor 2B

Similarly to glibenclamide, the administration of another sulfonylurea, tolbutamide (100  $\mu\text{mol/L}$ ), was able to stimulate fluid secretion in IBDUs (Figure 1A and Table 1). Preincubation with diazoxide (100  $\mu\text{mol/L}$ ), a classic SUR inhibitor, inhibited glibenclamide-stimulated secretion (Figure 1C and Table 1), consistent with the functional involvement of the SUR. Indeed, RT-PCR of mRNA extracted from immunopurified cholangiocytes revealed gene expression of SUR2B, the most widely expressed SUR isoform (Figure 3A), and of Kir 6.1 (Figure 3B), a protein belonging to a family of  $\text{K}^+_{\text{ATP}}$  channels associated with SUR.

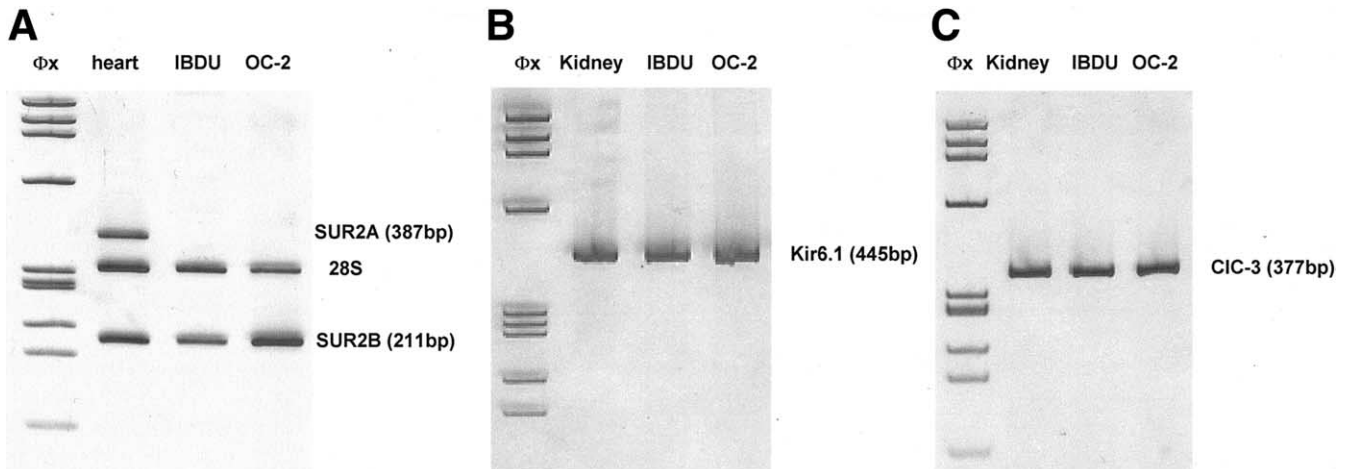


**Figure 3.** Gene expression of the SUR2B receptor, of the Kir 6.1  $K^+_{ATP}$  channel, and of the CLC-3  $Cl^-$  channel in IBDUs and in immunopurified rat cholangiocytes (OC-2). (A) SUR2AB primers were designed to cross the 177-bp insert in the SUR2A DNA sequence that gives rise to alternative spliced SUR2 variants (the primer pairs should generate PCR fragments of 211 bp for rSUR2B and 387 bp for rSUR2A. In the heart (control tissue), both SUR2 variants are expressed, whereas in IBDUs and OC-2 only the SUR 2B variant is expressed; the ribosomal fraction 28S was used as a housekeeping gene. (B) Kir 6.1, but not Kir 6.2 (data not shown), isoform PCR products are present in IBDUs and OC-2 cells. (C) The CLC-3  $Cl^-$  channel is expressed in IBDUs and OC-2 cells; kidney tissue was used as a positive control.

### Stimulation of Ductal Choleresis in Cholangiocytes Is Independent From Depolarization and Stimulation of $Ca^{2+}$ Transients

In  $\beta$ -cells, sulfonylureas trigger insulin secretion by stimulating exocytotic events. Therefore, we tested the effects of several agents known to inhibit vesicular transport in the liver<sup>24–26</sup> on glibenclamide-mediated choleresis: the microtubule-disrupting agent colchicine (50  $\mu$ mol/L; but not the inactive analogue  $\gamma$ -lumicolchicine), 2 phosphoinositol-3' kinase inhibitors (wortmannin 100 nmol/L and LY294002 50  $\mu$ mol/L), and *N*-ethylmaleimide (NEM; 1 mmol/L; an inhibitor of Soluble *N*-ethylmaleimide-sensitive factor attachment protein receptor (SNARE) proteins required to permit vesicles to fuse with plasma membrane). All significantly inhibited glibenclamide-induced secretion in IBDUs (Figure 4A and Table 1). Taken together, these results indicate that glibenclamide stimulates vesicle exocytosis in cholangiocytes.

In pancreatic  $\beta$ -cells, the binding of glibenclamide to SUR inhibits the function of  $K^+_{ATP}$  channels. The resulting cell depolarization causes  $Ca^{2+}$  influx through L-type  $Ca^{2+}$  channels, and the increase in intracellular  $[Ca^{2+}]$  stimulates exocytosis of insulin. However, in IBDUs, cell depolarization induced by depolarizing concentrations of extracellular  $K^+$  (40 mmol/L)<sup>4</sup> or by barium (5 mmol/L) and TEA (10 mmol/L) (2 well-known  $K^+$ -channel inhibitors) did not stimulate secretion in IBDUs (Figure 5A and Table 1). Furthermore, neither glibenclamide nor membrane depolarization increased

$Ca^{2+}$  in IBDUs (Figure 5B), whereas after ATP (10  $\mu$ mol/L) treatment, the expected  $Ca^{2+}$  response was recorded. The mechanism responsible for glibenclamide-induced secretion in cholangiocytes seems, therefore, to be similar to the  $Ca^{2+}$ -independent pathway that represents an additional mechanism through which sulfonylureas stimulate insulin secretion in pancreatic  $\beta$ -cells.<sup>23</sup> In this case, exocytosis of insulin-containing granules is dependent on the binding of glibenclamide to granular binding sites and is triggered by increasing osmotic forces inside the secretory granules induced by the cooperation of a V-type  $H^+$ -adenosine triphosphatase (ATPase) and an accompanying shunt conductance provided by a CLC-3  $Cl^-$  channel. Consistent with the predictions of this latter model, glibenclamide-induced fluid secretion was inhibited by V-type  $H^+$ -ATPase inhibitors such as bafilomycin A (1  $\mu$ mol/L) and vanadate (100  $\mu$ mol/L; Figure 4B and Table 1). Also, glibenclamide-induced secretion was inhibited by niflumic acid, an inhibitor of  $Cl^-$  channels, including CLC-3, the gene expression of which was detected by RT-PCR in immunopurified cholangiocytes (Figure 3C).

### Capacitance and Conductance Measurements on Isolated Cholangiocytes

To directly assess the possibility of vesicular release, we performed patch-clamp experiments on immunopurified cholangiocytes. Single cells measuring on average  $7.06 \pm 1.3 \mu$ m in diameter ( $n = 28$ ) were studied; this size equates to a simple spherical membrane surface area of  $156 \mu$ m<sup>2</sup> (Figure 6A). Our measured diameter is

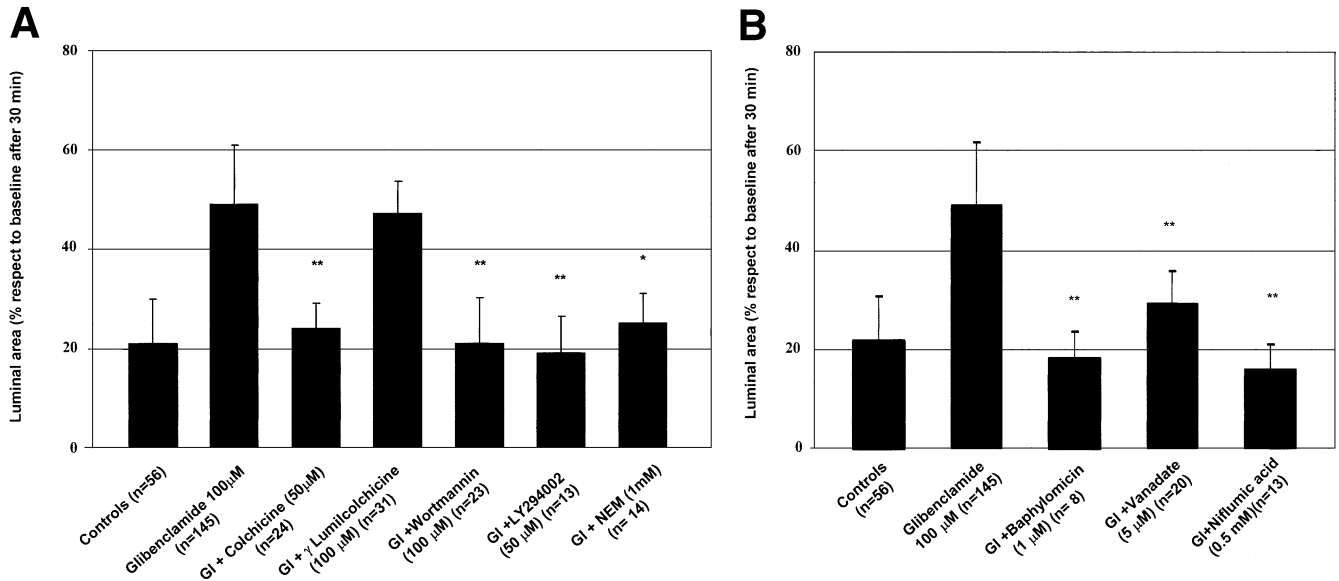


**Figure 4.** The choleric effect of glibenclamide in IBDUs is mediated by vesicular transport and is inhibited by V-type H<sup>+</sup> ATPase and CLC-3 Cl<sup>-</sup> channel blockers. (A) Inhibition by colchicine, phosphoinositol-3' kinase inhibitors (wortmannin and LY294002), and the SNARE inhibitor NEM. (B) Inhibition by V-type H<sup>+</sup> ATPase inhibitors (bafilomycin and vanadate) and of CLC-3 inhibitors (niflumic acid). Columns represent the percentage of luminal area expansion with respect to baseline 30 minutes after the administration of glibenclamide (mean ± SD). \*P < .01; \*\*P < .001 vs glibenclamide. Gl, glibenclamide.

smaller than that found in other reports<sup>27</sup> that used cholangiocytes isolated from bile duct-ligated rats, rather than from normal ones, and is consistent with the size reported by Kanno et al<sup>13</sup> for small duct cholangiocytes. The initial control cell diameter was  $7.47 \pm 0.91$

μm, and C<sub>m</sub> was  $2.22 \pm 1.1$  pF (n = 5). On the basis of recent estimates of specific C<sub>m</sub> (0.005 pF/μm<sup>2</sup>),<sup>28</sup> this C<sub>m</sub> measurement exceeds the expected value of 0.87 pF and indicates that substantial cell membrane folding exists. Even with the more commonly used translation factor of

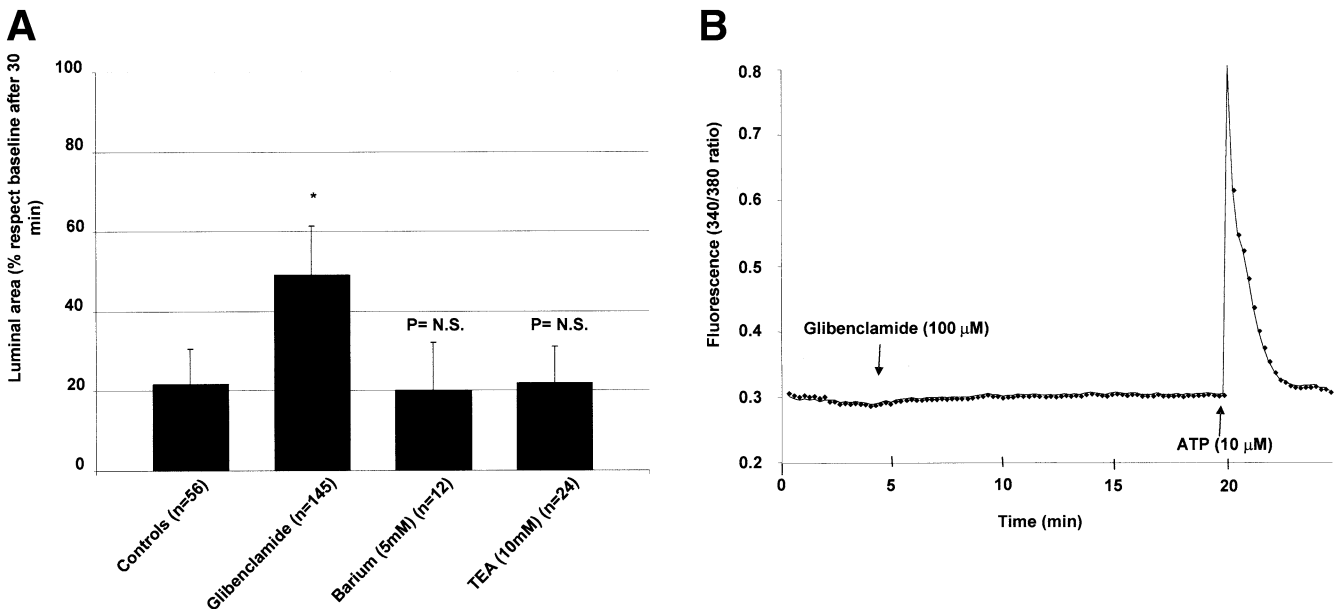


**Figure 5.** (A) Effects of depolarization on luminal expansion in IBDUs. Depolarizing concentrations of barium and of TEA did not stimulate secretion in IBDUs. Columns represent the percentage of luminal area expansion with respect to baseline after 30 minutes of stimulus administration (mean ± SD). (B) Effect of glibenclamide on intracellular Ca<sup>2+</sup> levels. A representative tracing is shown of 22 similar experiments showing changes in the ratio of the 2 wavelengths of FURA-2 induced by the administration of glibenclamide. Glibenclamide did not increase intracellular [Ca<sup>2+</sup>] in IBDUs, whereas administration of ATP induced the expected Ca<sup>2+</sup> increase. Similar experiments (n = 10) were performed by depolarizing the cells with TEA (10 mmol/L), and no significant changes in intracellular [Ca<sup>2+</sup>] were found. N.S., not significant.

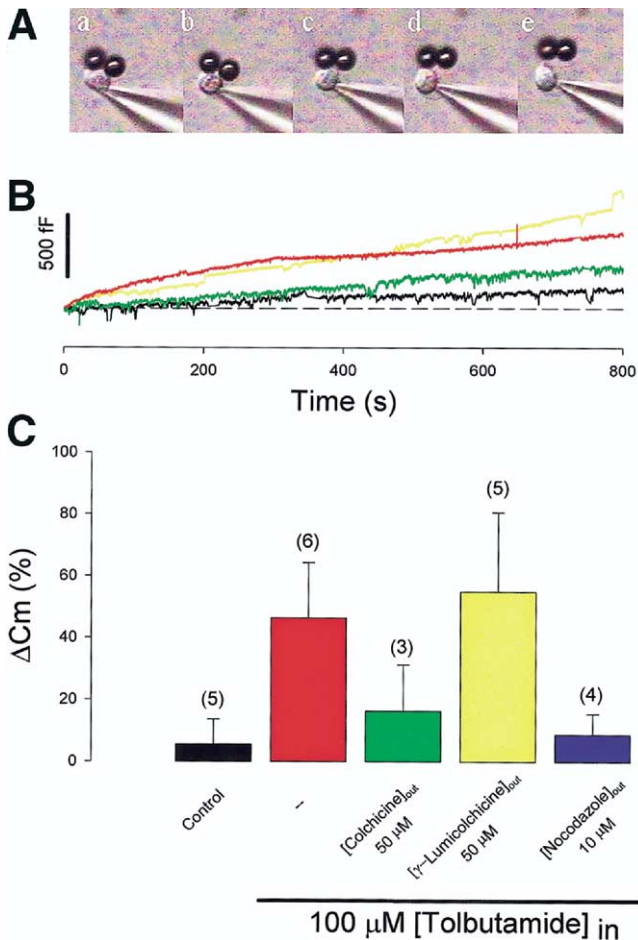


**Figure 6.** Whole-cell capacitance measurements in cholangiocytes. (A) Isolated cholangiocyte with 2 magnetic beads (diameter, 4.5  $\mu\text{m}$ ) attached to the cell membrane. Images a–e were captured at 5 minutes 12 seconds, 7 minutes 10 seconds, 10 minutes 24 seconds, 13 minutes 3 seconds, and 16 minutes 34 seconds after the establishment of whole-cell conditions, respectively. Note the gradual upward shift of beads as the cell swells. The change in surface area is smaller than it appears. This can be appreciated as follows. The initial diameter of the cell at 5 minutes 12 seconds is 7  $\mu\text{m}$ , giving an apparent area of 153  $\mu\text{m}^2$ ; the final diameter is 10.7  $\mu\text{m}$ , giving an area of 373  $\mu\text{m}^2$ . The initial capacitance is 1.12 pF, which equates to 224  $\mu\text{m}^2$ . Thus, the membrane at the beginning is highly folded, and the diameter is underestimated.<sup>28</sup> The capacitance at 16 minutes 34 seconds is 1.81 pF, which equates to 362  $\mu\text{m}^2$  and corresponds well to the measured diameter of the inflated cell. (B) Example  $C_m$  recordings for 4 different cells after the establishment of whole-cell conditions; colors correspond to color-coded treatments in (C). Initial capacitance for individual cells was as follows: black, 1.611 pF; yellow, 0.716 pF; red, 1.655 pF; and green, 1.152 pF. (C) Bar graph depicting average results (with SD error lines) for the different cell treatments. See Materials and Methods for details. The number of cells is indicated. Tolbutamide significantly enhanced  $C_m$  increases over control-level increases ( $P < .05$ ). Colchicine and nocodazole treatment significantly suppressed  $C_m$  changes compared with tolbutamide and  $\gamma$ -lumicolchicine treatment ( $P < .05$ ).

0.01 pF/ $\mu\text{m}^2$ ,  $C_m$  measurements suggest significant membrane folding that is not resolved at the light-microscopic level.  $C_m$  measurements in control cells were quite stable for tens of minutes (Figure 6B).

After establishment of whole-cell recording with pipettes containing tolbutamide (100  $\mu\text{mol/L}$ ),  $C_m$  increased over the course of several minutes (Figure 6B). Concomitantly, cells swelled; this was easily discerned by the movement of the membrane-bound magnetic beads that followed the contour of the expanding cell outline (Figure 6A).  $C_m$  eventually leveled off; at steady state, increases of 56% and 50% were found (Figure 6C). The preincubation of cholangiocytes with either colchicine (50  $\mu\text{mol/L}$  for 30 minutes) or nocodazole (10  $\mu\text{mol/L}$  for 60 minutes) blocked the increase in capacitance caused by tolbutamide. However, an inactive form of colchicine, namely,  $\gamma$ -lumicolchicine (50  $\mu\text{mol/L}$ ; 30 minutes), was unable to block the effects of tolbutamide (Figure 6C). We also found cells to swell during these treatments, so the increase in cell size (and, possibly, surface area) may not solely underlie the capacitance increases that we found (see Discussion).

Membrane conductance and holding current remained stable during recordings of control cells and cells treated with tolbutamide. Current–voltage relations showed linear, time-invariant currents (Figure 7), which in the example cell actually decreased slightly during tolbutamide treatments. For 6 cells, the membrane conductance at 0 mV was unaffected by tolbutamide during the time when  $C_m$  levels significantly increased (0 minutes,  $0.985 \pm 0.23$  nS; 10 minutes,  $1.15 \pm 0.3$  nS; paired  $t$  test;  $P = .158$ ). Thus, in our isolated cholangiocytes, we

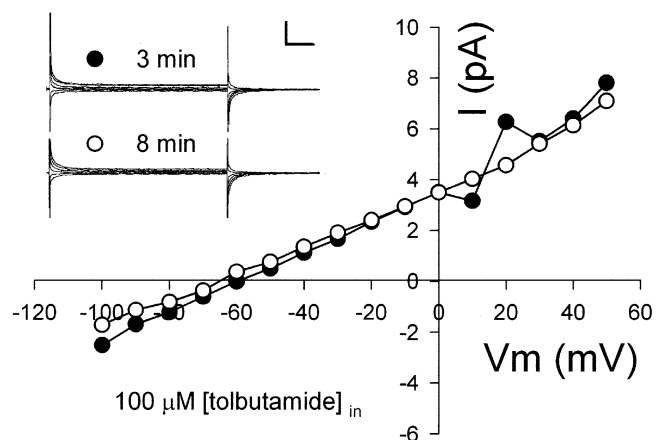


**Figure 7.** Whole-cell conductance measurements in cholangiocytes. I–V curves at 3 minutes (●) and 8 minutes (○) after the establishment of whole-cell conditions with 100  $\mu\text{mol/L}$  tolbutamide-containing pipette solution. Only a slight decrease in chord conductance was observed in this example. (Inset) Corresponding current traces at selected voltages (200-millisecond pulse duration) of –100, –70, –40, –10, 20, and 50 mV. Note linear, time-independent currents. Voltage at 0 current was stable and negative, near –60 mV; calculated reversal potentials for K and Cl were –86 and –34 mV, respectively. Scale: 40 pA, 31 milliseconds. Traces were filtered at 500 Hz with a digital gaussian filter.

found no evidence for a plasma membrane  $\text{Cl}^-$  conductance augmented by the increase in  $C_m$ .

### Glibenclamide Stimulates Bile Flow in Isolated Perfused Mouse Liver and Fluid Secretion in Isolated Bile Duct Units From Cystic Fibrosis Transmembrane Conductance Regulator Knockout Mice

Because glibenclamide is a known CFTR inhibitor, our data thus far suggest that the choleric effect of glibenclamide is mediated by a CFTR-independent mechanism that would likely be maintained in CF. To address this possibility, we tested the effect of glibenclamide in isolated perfused mouse liver and in IBDUs from mice knocked out for CFTR (B6.129P2-Cftr<sup>tm1Unc</sup>). In isolated perfused mouse liver, glibenclamide increased bile flow in wild-type mice as well as in CFTR knockout mice, and, interestingly, the increase in bile flow was significantly higher in CFTR knockout mice (Figure 8). In IBDUs isolated from 4 wild-type and 4 heterozygous mice, the administration of forskolin (10  $\mu\text{mol/L}$ ) or secretin (50 nmol/L) significantly increased the luminal area (wild-type—forskolin,  $68\% \pm 19\%$ ,  $n = 42$ ; secretin,  $62\% \pm 17\%$ ,  $n = 39$ ,  $P < .01$  vs controls,  $12\% \pm 6\%$ ,  $n = 36$ ; heterozygous—forskolin,  $58 \pm 13\%$ ,  $n = 51$ ; secretin,  $57\% \pm 20\%$ ,  $n = 24$ ;  $P < .01$  vs controls,  $14\% \pm 6\%$ ,  $n = 31$ ). In IBDUs isolated from 5 homozygous CFTR knockout mice ( $-/-$ ), the effects of forskolin and of secretin were significantly inhibited

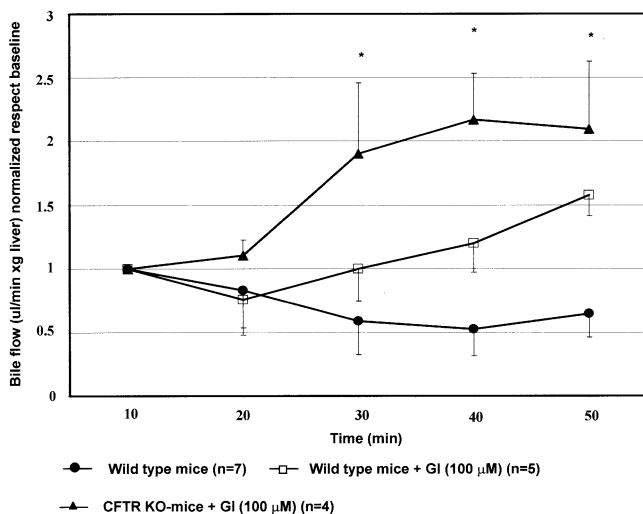


**Figure 8.** Glibenclamide stimulates bile flow in wild-type and CFTR knockout mice. Glibenclamide stimulates bile flow in isolated perfused mouse livers from wild-type and CFTR knockout mice. Bile flow was significantly increased ( $*P < .001$ ) in wild-type and CFTR knockout mouse livers perfused with glibenclamide (100  $\mu\text{mol/L}$ ) with respect to wild-type mice. Bile flow is expressed as microliters of bile secreted in 1 minute and normalized for liver weight. GI, glibenclamide.

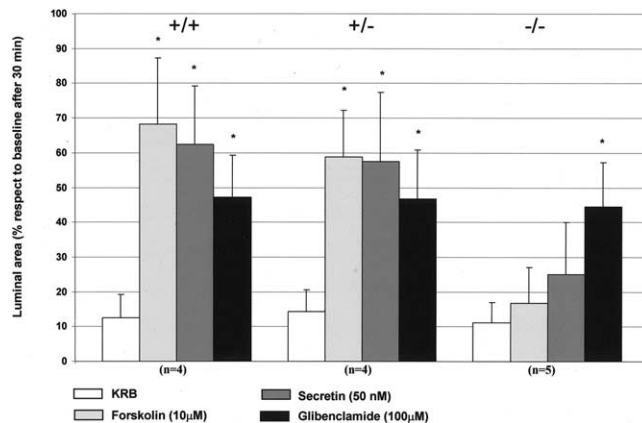


**Figure 9.** The choleric effect of glibenclamide is maintained in IBDUs isolated from CF mice. IBDUs were examined under control conditions for 10 minutes and then for an additional 30 minutes after the administration of glibenclamide, forskolin or secretin, or vehicle. Each luminal area was normalized by its initial value. Glibenclamide significantly ( $*P < .01$  vs controls) stimulated secretion in IBDUs isolated from wild-type (+/+), heterozygous (+/-), and homozygous (-/-) mice. Forskolin and secretin were able to significantly ( $*P < .01$ ) stimulate secretion only in wild-type and heterozygous, but not in homozygous, mice. KRB,  $\text{HCO}_3^-$ -containing Ringer buffer.

(forskolin,  $17\% \pm 10\%$ ,  $n = 54$ ; secretin,  $25\% \pm 17\%$ ,  $n = 41$ ;  $P < .001$  vs wild-type and heterozygous), thus indicating that the fundamental CF secretory defect was maintained in the liver of homozygous mice. Conversely, in CFTR knockout mice, the secretory effect of glibenclamide was maintained and was equal to that recorded in wild-type and heterozygous animals (Figure 9).

## Discussion

Strategies aiming at directly stimulating fluid secretion by cholangiocytes may be a useful approach to treat cholestasis in biliary tract diseases,<sup>2</sup> particularly in CF, in which reduced  $\text{Cl}^-$  and fluid secretion into the lumen causes inspissation of bile and chronic liver damage. To this end, we have studied the molecular mechanisms underlying the choleric effects of glibenclamide. The interest in this compound derives from previous studies by Nathanson et al,<sup>4</sup> which showed that glibenclamide, a known CFTR inhibitor, paradoxically stimulates bile flow at the level of cholangiocytes.

Because the mechanism of glibenclamide-induced choleresis was not clarified, we sought to investigate these mechanisms in more detail. Given the inhibitory effects of bumetanide on glibenclamide-induced cholangiocyte secretion, a direct stimulation of  $\text{Cl}^-$  uptake by the NKCC1 cotransporter<sup>15</sup> was proposed as a possible explanation.<sup>4</sup> In this study, we have measured the effects of glibenclamide on  $\text{Na}^+/\text{K}^+2\text{Cl}^-$  activity, and, contrary to the previous hypothesis,<sup>4</sup> we could find no

evidence of NKCC1 stimulation. Our data also show that polarized cholangiocytes<sup>7-9</sup> are not able to transport glibenclamide into the apical lumen and that this stimulation of secretion is not due to an osmotic choleresis.

After binding to a specific receptor (SUR), sulfonylureas stimulate an exocytotic release of insulin from pancreatic  $\beta$ -cells.<sup>5,29</sup> The following observations suggest that the choleric effect of glibenclamide on cholangiocytes may also be due to a receptor-mediated mechanism: (1) tolbutamide, another sulfonylurea, was able to induce luminal expansion in IBDUs to a similar extent; (2) the mRNA for SUR2B was expressed in immunopurified cholangiocytes; and (3) diazoxide, a known SUR inhibitor, significantly inhibited the secretory effect of glibenclamide. Our data also indicate that, similar to their effects on pancreatic  $\beta$ -cells,<sup>17,29</sup> sulfonylureas are likely to stimulate fluid secretion via vesicular transport in cholangiocytes. In fact, tolbutamide induced an increase in  $C_m$  in immunisolated cholangiocytes; in addition, glibenclamide-induced secretion and/or the increase in  $C_m$  was inhibited by compounds known to block vesicular transport in the liver, such as colchicine, nocodazole, and wortmannin,<sup>24-26</sup> and by NEM. These compounds act through different mechanisms; whereas colchicine and nocodazole are microtubule inhibitors, wortmannin is a phosphoinositol-3' kinase inhibitor, and NEM blocks the NEM-sensitive fusion protein.<sup>30,31</sup> Although none of them can be considered a specific inhibitor of vesicular exocytosis, their consistent inhibitory effect on glibenclamide choleresis and on  $C_m$  changes provides strong evidence that glibenclamide stimulates vesicle exocytosis in cholangiocytes.

In the pancreatic  $\beta$ -cell, SUR complexes with Kir 6.x (a Kir sensitive to intracellular concentration of ATP [ATP]<sub>i</sub>). In these cells, closure of the  $K_{ATP}$  channel induced by glibenclamide interaction with SUR depolarizes the cell, favoring  $Ca^{2+}$  influx via L-type  $Ca^{2+}$  channels.<sup>32</sup> Although expression of the mRNA of the Kir 6.1  $K_{ATP}$  channel isoform was detectable in immunopurified cholangiocytes (Figure 3B), neither the  $K^+$  channel inhibitor TEA nor maneuvers aimed at inducing membrane depolarization in cholangiocytes (barium or high  $K^+$ )<sup>4</sup> were able to induce luminal expansion in IBDUs. Also, in patch-clamp experiments, depolarization did not induce vesicular release; furthermore, neither the administration of glibenclamide nor membrane depolarization increased intracellular  $Ca^{2+}$  levels. This is in clear contrast to the 450 nmol/L intracellular [ $Ca^{2+}$ ] increase induced by depolarization in  $\beta$ -cells.<sup>33</sup> Altogether, these data suggest that, in cholangiocytes, glibenclamide stimulates secretion via a mechanism that is independent from depolarization and  $Ca^{2+}$  transients.

In pancreatic  $\beta$ -cells, sulfonylureas are also able to potentiate insulin secretion by acting directly on the exocytotic machinery. Ninety percent of the high-affinity sulfonylurea binding sites in the  $\beta$ -cell are intracellular and seem to colocalize with the insulin-containing secretory granules.<sup>25,26</sup> Recent studies have also shown that recombinant green fluorescent protein-tagged SUR and Kir colocalize with fluorescent glibenclamide in insulin-containing granules.<sup>34</sup> Furthermore, it has been shown that sulfonylureas, being weak acids, can cross biological membranes by diffusion,<sup>35</sup> thus inducing a pHi decrease similar to the one originally described by Nathanson et al<sup>4</sup> in cholangiocytes. Several studies have provided evidence indicating that intracellular binding of sulfonylureas activates a DIDS- and niflumic acid-sensitive CLC-3  $Cl^-$  channel operating in conjunction with a bafilomycin-sensitive V-type  $H^+$ -ATPase. The resulting  $Cl^-$  and  $H^+$  influx stimulates the exocytotic machinery and insulin discharge in a depolarization and  $Ca^{2+}$  independent way.<sup>17,36,37</sup> In fact, a low granular pH promotes conformational changes in SNARE proteins, making them more fusogenic.<sup>29</sup> Our data in cholangiocytes are consistent with this mechanism; in fact, (1) glibenclamide administration does not increase intracellular [ $Ca^{2+}$ ] levels; (2) membrane depolarization does not stimulate cholangiocyte secretion; (3) CLC-3 mRNA was detected in cholangiocytes; (4) DIDS, a generic inhibitor of  $Cl^-$  channels, and niflumic acid, which inhibits CLC-3, blocked the choleric response to glibenclamide; and (5) the V-type  $H^+$ -ATPase inhibitors bafilomycin A1 and vanadate significantly reduced the secretory response to glibenclamide. Altogether, these data suggest the presence in cholangiocytes of a cAMP- and  $Ca^{2+}$ -independent secretory mechanism that is stimulated by sulfonylureas and requires functional exocytotic machinery.

Our capacitance measurements provide further evidence that tolbutamide promotes an increase in cell-surface area; the dependence of this effect on microtubule stability argues for vesicular fusion with the plasma membrane.<sup>38</sup> Increases in  $C_m$  of approximately 50% were found, similar to our luminal area measurements in IBDUs, and although this may seem large, a complete vesicular release in bile ductal cells of the pig increased the membrane surface area by >100%.<sup>39</sup> Actually, an increase in capacitance may arise from several sources, including an increase in membrane surface area due to vesicular fusion and swelling of the cell with attendant thinning of the membrane and unraveling of membrane folds (eg, microvilli). Thinning of the membrane caused by membrane stretch is expected to increase specific  $C_m$ , and the resulting increase in whole-cell capacitance can-

not be distinguished electrically from actual membrane accrual. Additionally, tight folding of the membrane may initially limit the accessibility of voltage perturbation across those membranes, and after cell swelling and unraveling, these membranes may then be fully excited and contribute more to  $C_m$  measurements. We found that cells readily swelled during our recording and, indeed, shifted the attached magnetic beads (Figure 6A). Although the microtubule destabilizers may be thought to specifically inhibit vesicular release in cholangiocytes,<sup>38</sup> they may also somehow affect the other potential mechanisms of  $C_m$  increase. Thus, we cautiously hypothesize that at least a component of  $C_m$  increase results from vesicular fusion.

Usually we held the cell membrane potential at zero voltage during capacitance measurements, because we observed that cells were not maintained for prolonged periods of time when they were held at negative potentials. Despite this depolarized holding potential, control cells did not show capacitance increases as might have occurred if an influx of extracellular  $Ca^{2+}$  via voltage-gated  $Ca^{2+}$  channels could induce exocytosis. Indeed, under our recording conditions, measurements do not show inward currents typical of non-inactivating L-type  $Ca^{2+}$  channels.

We did not find significant changes in membrane conductance during tolbutamide treatments. Indeed, our isolated cells, before and after these treatments, showed only small linear, time-independent currents, similar to 1 pattern of 3 found by Fitz et al.<sup>27</sup> Perhaps our isolation technique favored a particular cell subpopulation. The holding current was remarkably stable during our treatments, and current-voltage relations confirmed these measurements, showing that changes in ionic conductance did not necessarily accompany  $C_m$  increases. Although we observed that secretion in IBUs could be inhibited by  $Cl^-$  channel blockers, it should be noted that our whole-cell voltage-clamp measurements are unable to assess channel activity within intracellular membrane compartments, such as vesicles; of course, blockers may work at this level. As already shown,<sup>37,40</sup>  $ClC-3$  channels provide an electrical shunt pathway that permits vesicle acidification by the vacuolar pump before vesicular release. This scenario favors a fluid-phase type of secretory activity in our cholangiocyte preparation.

The transport functions of the biliary epithelium are regulated by different gastrointestinal hormones that stimulate either secretory or absorptive mechanisms.<sup>1</sup> Secretin, the principal stimulatory hormone, increases ductular choleresis through cAMP/protein kinase A-dependent stimulation of  $Cl^-$  efflux and  $HCO_3^-$  secretion

through the coordinated actions of CFTR and the anion exchanger isoform 2  $Cl^-/HCO_3^-$  exchanger, both located at the apical pole of the cells.<sup>41,42</sup>  $Cl^-$  efflux into the bile can also be mediated by  $Ca^{2+}$ -dependent  $Cl^-$  channels stimulated by binding of extracellular ATP to P2Y2 purinergic receptors located at the apical pole of cholangiocytes.<sup>3,23</sup> In addition, a substantial amount of evidence indicates that stimulation of vesicular transport and fusion plays a role in cholangiocyte secretion. In vivo and in vitro studies using fluid-phase markers have shown that cholangiocytes are capable of microtubule-dependent fluid-phase transcytotic transport from the basolateral to the apical domains.<sup>10,38,43</sup> Furthermore, cholangiocytes possess a dense population of subapical vesicles that undergo a high rate of constitutive exocytosis<sup>44</sup> that can be stimulated by osmotic stress and by cAMP. Cyclic AMP stimulates the exocytosis of acridine orange in cholangiocytes<sup>38</sup> and the apical insertion of vesicles containing aquaporins and ion transporters (such as CFTR and anion exchanger isoform 2) as a means of achieving rapid regulation of biliary ion and fluid transport.<sup>45</sup>

The choleric effect of glibenclamide is a paradox; in fact, because it is a known inhibitor of CFTR, one would expect glibenclamide to inhibit secretion. Thus, the major finding of our study, which is of potential therapeutic relevance, is that sulfonylureas possess the ability to stimulate cholangiocyte secretion, thus promoting a novel cAMP-,  $Ca^{2+}$ -, and depolarization-independent exocytotic mechanism, and that this effect is preserved and even more active in experimental animals defective for CFTR. An important line of research in CF aims at finding small molecules able to stimulate fluid secretion in CFTR-defective cells and focuses on compounds able to function as molecules that (1) can serve as chaperones for CFTR, (2) can activate the mutated CFTR, and (3) can stimulate  $Ca^{2+}$ -dependent  $Cl^-$  conductances.

Direct transfer of these observations to human therapy is not likely, because the  $K_d$  for the choleric effects of glibenclamide is approximately 9  $\mu\text{mol/L}$ ,<sup>4</sup> a concentration that may result in hypoglycemia. However, our data represent an important proof of concept; the identification of a compound able to stimulate bile secretion independently of CFTR and the 2 major signaling pathways ( $Ca^{2+}$  and cAMP) is of major general interest. Sulfonylureas may thus represent model compounds to design drugs for conditions characterized by a failure in cAMP-dependent secretion (such as CF-related liver disease) and possibly other cholestatic conditions in which a defect in  $Ca^{2+}$  signaling is present.<sup>46</sup>

## References

- Strazzabosco M. New insights into cholangiocyte physiology. *J Hepatol* 1997;27:945–952.
- Ferenchak AP, Sokol RJ. Cholangiocyte biology and cystic fibrosis liver disease. *Semin Liver Dis* 2001;21:471–487.
- Zsembery A, Jessner W, Spirli C, Strazzabosco M, Graf J. Correction of CFTR malfunction and stimulation of  $\text{Ca}^{2+}$ -activated  $\text{Cl}^-$  channels restore  $\text{HCO}_3^-$  secretion in cystic fibrosis bile ductular cells. *Hepatology* 2002;35:95–104.
- Nathanson MH, Burgstahler AD, Mennone A, Dranoff JA, Rios-Velez L. Stimulation of bile duct secretion by glibenclamide in normal and cholestatic rat liver. *J Clin Invest* 1998;101:1–12.
- Doyle ME, Egan JM. Pharmacological agents that directly modulate insulin secretion. *Pharmacol Rev* 2003;55:105–131.
- Spirli C, Nathanson MH, Fiorotto R, Duner E, Denson LA, Sanz JM, Di Virgilio F, Casagrande F, Strazzabosco M. Pro-inflammatory cytokines inhibit secretion in rat bile duct epithelium. *Gastroenterology* 2001;121:156–169.
- Spirli C, Granato A, Zsembery A, Anglani F, Okolicsanyi L, La Russo NF, Crepaldi G, Strazzabosco M. Functional polarity of  $\text{Na}^+/\text{H}^+$  and  $\text{Cl}^-/\text{HCO}_3^-$  exchangers in a rat cholangiocytes cell line. *Am J Physiol* 1998;275:G1236–G1245.
- Vroman B, La Russo NF. Development and characterization of polarized primary cultures of rat intrahepatic bile duct epithelial cells. *Lab Invest* 1996;74:303–313.
- Lazaridis KN, Pham L, Vroman B, de Groen PC, LaRusso NF. Kinetic and molecular identification of sodium-dependent glucose transporter in normal rat cholangiocytes. *Am J Physiol* 1997;272:G1168–G1174.
- Benedetti A, Marucci L, Bassotti C, Mancini R, Contucci S, Jezequel AM, Orlandi F. Tubulovesicular transcytotic pathway in rat biliary epithelium: a study in perfused liver and isolated intrahepatic bile duct. *Hepatology* 1993;18:422–432.
- Mennone A, Alvaro D, Cho W, Boyer JL. Isolation of small polarized bile duct units. *Proc Natl Acad Sci U S A* 1995;92:6527–6531.
- Spirli C, Fabris L, Duner E, Fiorotto R, Ballardini G, Roskams T, La Russo NF, Sonzogni A, Okolicsanyi L, Strazzabosco M. Cytokine-stimulated, nitric oxide production inhibit adenylyl cyclase and cAMP-dependent secretion in cholangiocytes. *Gastroenterology* 2003;124:737–753.
- Kanno N, Le Sage G, Glaser S, Alvaro D, Alpini G. Functional heterogeneity of the intrahepatic biliary epithelium. *Hepatology* 2000;31:555–561.
- Strazzabosco M, Mennone A, Boyer JL. Intracellular pH regulation in isolated rat bile duct epithelial cells. *J Clin Invest* 1991;87:1503–1512.
- Insering P, Jacoby SC, Payne JA, Forbush B III. Comparison of Na-K-Cl cotransporters. *J Biol Chem* 1998;273:11295–11301.
- Brini M, De Giorgi F, Murgia M, Marsault R, Massimino ML, Cantini M, Rizzuto R, Pozzan T. Subcellular analysis of  $\text{Ca}^{2+}$  homeostasis in primary cultures of skeletal muscle myotubes. *Mol Biol Cell* 1997;8:129–143.
- Barg S, Renstrom E, Berggren PO, Bertorello A, Bokvost K, Braun M, Eliasson L, Holmes WE, Kohler M, Rorsman P, Thevenod F. The stimulatory action of tolbutamide on  $\text{Ca}^{2+}$ -dependent exocytosis in pancreatic  $\beta$  cells is mediated by a 65-kDa mdr-like P-glycoprotein. *Proc Natl Acad Sci U S A* 1999;96:5539–5544.
- Santos-Sacchi J, Kakehata S, Takahashi S. Effects of membrane potential on the voltage dependence of motility-related charge in outer hair cells of the guinea-pig. *J Physiol* 1998;510:225–235.
- Santos-Sacchi J. Determination of cell capacitance using the exact empirical solution of  $dY/dC_m$  and its phase angle. *Biophys J* 2004;87:714–727.
- Santos-Sacchi J. Isolated supporting cells from the organ of Corti: some whole cell electrical characteristics and estimates of gap junctional conductance. *Hear Res* 1991;52:89–98.
- Snouwaert JN, Brigman KK, Latour AM, Malouf NN, Boucher RC, Smithies O, Koller BH. An animal model for cystic fibrosis made by gene targeting. *Science* 1992;257:1083–1088.
- Oude-Elferink RPJ, Ottenhoff R, van Wijland M, Smit JJM, Schinkel AH, Groen AK. Regulation of biliary lipid secretion by mdr2 P-glycoprotein in the mouse. *J Clin Invest* 1995;95:31–38.
- Zsembery A, Spirli C, Granato A, LaRusso NF, Okolicsanyi L, Crepaldi G, Strazzabosco M. Purinergic regulation of acid/base transport in human and rat biliary epithelial cell lines. *Hepatology* 1998;28:914–920.
- Dallenbach A, Renner EL. Colchicine does not inhibit secretin-induced choleresis in rats exhibiting hyperplasia of bile ductules: evidence against a pivotal role of exocytotic vesicle insertion. *J Hepatol* 1995;22:338–348.
- Sato SB, Taguchi T, Yasmashina S, Toyama S, Wortmannin and  $\text{Li}^+$  specifically inhibit clathrin-independent endocytic internalization of bulk fluid. *J Biochem* 1996;119:887–897.
- Folli F, Alvaro D, Gigliozzi A, Bassotti C, Kahn RC, Pontiroli AE, Capocaccia L, Jezequel AM, Benedetti A. Regulation of endocytic-transcytotic pathways and bile secretion by phosphatidylinositol 3-kinase in rats. *Gastroenterology* 1997;113:954–965.
- Fitz JG, Basavappa S, McGill J, Melhus O, Cohn JA. Regulation of membrane chloride currents in rat bile-duct epithelial-cells. *J Clin Invest* 1993;91:319–328.
- Solsona C, Innocenti B, Fernandez JM. Regulation of exocytotic fusion by cell inflation. *Biophys J* 1998;74:1061–1073.
- Thevenod F. Ion channels in secretory granules of the pancreas and their role in exocytosis and release of secretory proteins. *Am J Physiol* 2002;283:C651–C672.
- Galli T, Zahraoui A, Vaidyanathan VV, Raposo G, Tian JM, Karin M, Niemann H, Louvard D. A novel tetanus neurotoxin-insensitive vesicle-associated membrane protein in SNARE complexes of the apical plasma membrane of epithelial cells. *Mol Biol Cell* 1998;9:1437–1448.
- Xu T, Ashery U, Burgoyne RD, Neher E. Early requirement for  $\alpha$ -SNAP and NSF in the secretory cascade in chromaffin cells. *EMBO J* 1999;18:3293–3304.
- Ashcroft FM, Gribble FM. Tissue-specific effects of sulfonylureas: lessons from studies of cloned  $\text{K}_{\text{ATP}}$  channels. *J Diabetes Complications* 2000;14:192–196.
- Abrahamsson H, Berggren PO, Rorsman P. Direct measurements of increased free cytoplasmic  $\text{Ca}^{2+}$  in mouse pancreatic beta-cells following stimulation by hypoglycemic sulfonylureas. *FEBS Lett* 1985;190:21–24.
- Geng X, Lehong L, Watkins S, Robbins PD, Drain P. The insulin secretory granule is the major site of  $\text{K}_{\text{ATP}}$  channels of the endocrine pancreas. *Diabetes* 2003;52:767–776.
- Kamp F, Kizilbash N, Corkey B, Berggren PO, Hamilton J. Sulfonylureas rapidly cross phospholipid bilayer membranes by a free-diffusion mechanism. *Diabetes* 2003;52:2526–2531.
- Renstrom E, Barg S, Thevenod F, Rorsman P. Sulfonylurea-mediated stimulation of insulin exocytosis via an ATP-sensitive  $\text{K}^+$  channel-independent action. *Diabetes* 2002;51:S33–S36.
- Barg S, Huang P, Eliasson L, Nelson DJ, Obermuller S, Rorsman P, Thevenod F, Renstrom E. Priming of insulin granules for exocytosis by granular  $\text{Cl}^-$  uptake and acidification. *J Cell Sci* 2001;114:2145–2154.
- Kato A, Gores GJ, LaRusso NF. Secretin stimulates exocytosis in isolated bile duct epithelial cells by a cyclic AMP-mediated mechanism. *J Biol Chem* 1992;267:15523–15529.
- Buanes T, Grotmol T, Landsverk T, Raeder MG. Secretin empties bile-duct cell cytoplasm of vesicles when it initiates ductular  $\text{HCO}_3^-$  secretion in the pig. *Gastroenterology* 1988;95:417–424.

40. Hara-Chikuma M, Yang B, Sonawane ND, Sasaki S, Uchida S, Verkman AS. ClC-3 chloride channels facilitate endosomal acidification and chloride accumulation. *J Biol Chem* 2005;280:1241–1247.
41. Cohn JA, Strong TV, Picciotto MR, Nairn AC, Collins FS, Fitz JG. Localization of the cystic fibrosis transmembrane conductance regulator in human bile duct epithelial cells. *Gastroenterology* 1993;105:1857–1864.
42. Martinez-Ansò E, Castillo JE, Diaz J, Medina JF, Prieto J. Immunohistochemical detection of Cl<sup>-</sup>/HCO<sub>3</sub><sup>-</sup> anion exchanger in human liver. *Hepatology* 1994;19:1400–1406.
43. Benedetti A, Marucci L, Bassotti C, Guidarelli C, Jezequel AM. Brefeldin A inhibits the transcytotic vesicular transport of horseradish peroxidase in intrahepatic bile ductules isolated from rat liver. *Hepatology* 1995;22:194–201.
44. Doctor B, Dahl R, Fouassier L, Kilic G, Fitz JG. Cholangiocytes exhibit dynamic, actin-dependent apical membrane turnover. *Am J Physiol Cell Physiol* 2002;282:C1042–C1052.
45. Tietz PS, Marinelli RA, Chen XM, Huang B, Cohn J, Kole J, McNiven MA, Alper S, LaRusso NF. Agonist-induced coordinated trafficking of functionally related transport proteins for water and ions in cholangiocytes. *J Biol Chem* 2003;278:20413–20419.
46. Shibao K, Hirata K, Robert ME, Nathanson MH. Loss of inositol 1,4,5-trisphosphate receptors from bile duct epithelia is a common event in cholestasis. *Gastroenterology* 2003;125:1175–1187.

---

Received April 8, 2004. Accepted March 16, 2005.

Address requests for reprints to: Mario Strazzabosco, MD, PhD, Division of Gastroenterology, Ospedali Riuniti di Bergamo, Largo Barozzi, 1, 24128 Bergamo, Italy. e-mail: mstrazzabosco@ospedaliriuniti.bergamo.it; fax: (39) 035-26-6818.

Supported by Telethon (Grant E-873), by the Italian Cystic Fibrosis Research Foundation (Grant 2003) with the contribution of Fondazione Cariverona, by Ministero dell'Istruzione, Università e Ricerca (MIUR; cofinanziamento 2003; Grant 2003060498-001), by Fondazione San Martino, and by National Institutes of Health NIDCD Grant DC 000273 (J.S.-S.).